International Journal of Physics and Mathematics

**E-ISSN:** 2664-8644
**P-ISSN:** 2664-8636
IJPM 2025; 7(1): 10-23

www.physicsjournal.net
Received: 15-10-2024
Accepted: 21-11-2024

**SR Bhoyar**
Department of Mathematics, Phulsing Naik Mahavidyalaya, Pusad, Yavatmal, Maharashtra, India

**AV Pawar**
Department of Mathematics, Phulsing Naik Mahavidyalaya, Pusad, Yavatmal, Maharashtra, India

**Corresponding Author:**
**SR Bhoyar**
Department of Mathematics, Phulsing Naik Mahavidyalaya, Pusad, Yavatmal, Maharashtra, India

# Bianchi-type HDE Cosmological Models with Emergent Scenarios of Scale Factors under $f(R)$ Gravity

**SR Bhoyar and AV Pawar**

**DOI:** https://doi.org/10.33545/26648636.2025.v7.i1a.100

**Abstract**
This work is based on Bianchi-type II, VIII and IX HDE cosmological models with emergent scenarios of scale factor in $f(R)$ gravity. Here, we obtain the solution of field equations in the presence of HDE under some specific possible physical conditions. We have investigated the noninteracting and interacting GGPDE and DM. some physical and geometric feathers of models are also discussed.

**Keywords:** GGPDE, DM, Scale factor, HDE, $f(R)$ gravity.

## Introduction

Recent astronomical observations indicate that we live in an expanding and accelerating cosmos. These observations suggest that the cosmos is dominated by two dark components: dark matter and dark energy [1, 2, 3, 4, 5, 6]. Dark matter is a mysterious and invisible substance that accounts for approximately 27% of the total mass and energy content of the universe. Unlike regular matter (which comprises stars, planets, and everything we see), dark matter does not emit, absorb, or reflect light, rendering it invisible to electromagnetic radiation. Its existence is deduced from its gravitational effects on visible matter, radiation, and the large-scale structure of the cosmos.

The advancement of cosmology and gravitation is regarded as one of the twentieth century's scientific successes. Contemporary cosmic observational data [7] demonstrate that the expansion of the universe is accelerating. The cause of the far side of the measured acceleration is unclear, and it is sometimes referred to as the dark energy problem. Two methods have been proposed to explain this cosmic acceleration. The first approach is to propose and investigate several dynamical DE models, such as scalar field models (Quintessence, Phantom, and Quintom), Chaplygin gas [8], holographic [9, 10], Pilgrim [11], and DE models. The second technique is to change the Einstein-Hilbert action, which has been expanded to several alternative theories of gravity, $f(R)$ [12].

Sharif and Kausar [13] and Aditya et al. [14] discussed various nonvacuum Bianchi-type models in the $f(R)$ gravity theory. Reddy et al. [12] discussed Birkhoff's theorem in $f(R)$ the theory of gravity. Shamir [15] studied exact vacuum solutions of Bianchi type-I, III and Kantowski Sachs space-times in the metric version of $f(R)$ gravity. Yilmaz et al. [16] studied quark and strange quark matter in $f(R)$ gravity for Bianchi type-I and V-spaces. Reddy et al. [17], and Amir and Sattar [18] discussed different exact vacuum solutions of Bianchi spacetimes in terms of $f(R)$ gravity theory. Shamir [19] studied static plane-symmetric solutions in $f(R)$and $f(R,T)$ modified theories of gravity.

Saha et al. [20] highlighted the interplay between the spacetime metric's structure and the energy-momentum tensor's form, highlighting the significant influence of symmetry considerations in determining the physical characteristics of cosmological models. Katore et al. [21] investigate Bianchi type II VIII and IX string cosmological models in the context of $f(R)$ gravity. Singh et al. [22] discussed that the Bianchi type-II, VIII, and IX models have been investigated in scalar-tensor theories developed by Saez (1985), Saez and Ballester (1985), and Lau and Prokhovnik (1986). Santhi et al. [23] discussed the Tsallis Holographic Dark Energy (THDE) model in the context of general relativity (GR)

and spatially anisotropic Bianchi type-II, VIII, and IX universes. Using the linearly varying deceleration parameter (q) (LVDP) as a framework, the analysis explores the behavior and implications of THDE in these anisotropic spacetimes, shedding light on its role in cosmological evolution and deviations from isotropy. Quantum cosmology of the Bianchi VIII, IX LRS geometries. To explain the present accelerated stage of the Universe, a form of DE named the Veneziano ghost DE has been proposed. The energy density of the vacuum ghost is proportional to $\Lambda^3_{QCD}H$ and, where $\Lambda_{QCD}$ is the QCD mass scale and where $H$ is the Hubble parameter. This GDE has attracted the attention of researchers because its energy density $\rho_{DE}$ depends linearly on the Hubble parameter $H$ such as $\rho_{DE} = \tau H$ where $\tau$ is a constant with dimension [energy]$^3$ and is related to the Quantum Chromodynamics (QCD) mass scale. QCD describes strong interactions in nature. The general vacuum energy of the Veeziano ghost field in the QCD is $H$+O$(H)^2$ . The term $H^2$ occupies a significant position in the evolution of the early Universe, which acts as the early DE. By taking the term $H^2$ into account, one can achieve better agreement with observational data than the usual GDE which is known as generalized ghost dark energy (GGDE). The energy density of the generalized model is defined by $\rho_{DE} = (\tau H + \eta H^2)$ where $\eta$ is a constant. Wei proposed a new dark energy model called pilgrim DE (PDE) based on the speculation that black hole (BH) formation can be avoided through the strong repulsive force of the type of DE. GGDE has been modified in terms of the PDE as $\rho_{DE} = (\tau H + \eta H^2)^u$ where $u$ is a PDE parameter. The effective total negative pressure, which leads to a repulsive gravity in bulk viscosity, overcomes the attractive expansion of the universe. Many authors such as Wang, Shin'ichi Nojiri , Bali and Dave , and Bhoyar et al. discussed the role of non-viscous and viscous holographic dark energy (HDE) and dark matter (DM) for homogeneous anisotropic Bianchi type-II, type-VIII and type-IX cosmological models within the framework of maximal coupling between geometry and matter. $f(R)$ Theory of gravity.

Motivated by these investigations, in this paper, we focus our attention on the Bianchi type II, VIII, and IX HDE cosmological models with emergent scenarios of scale factors in $f(R)$ gravity. The plan of the paper is as follows: in section 2, we derive $f(R)$ gravity field equations for the Bianchi type II, VIII and IX metrics in the presence of GGPDE and matter. In section 3, solutions of the field equation are presented. The noninteracting and interacting models are discussed in sections 4 and 5. The paper ends with concluding remarks in section 6.

**Metric and Field Equations**

We consider the form's spatially homogeneous Bianchi type II, VIII and IX metrics.

$$ds^2 = -dt^2 + A^2[d\theta^2 + f^2(\theta)\,d\phi^2] + B^2[d\psi + h(\theta)\,d\phi]^2$$

Where (θ, ϕ, ψ) are the Eulerian angles and R and S are functions of t only. It represents.

Bianchi type-II if $f(\theta) = 1$ and $h(\theta) = \theta$

Bianchi type-VIII if $f(\theta) = cosh\theta$ and $h(\theta) = sinh\theta$

Bianchi type-IX if $f(\theta) = sin\theta$ and $h(\theta) = cos\theta$

The field equation of $f(R)$ gravity is obtained from the action principle.

$$S = \int \sqrt{-g}\left(\frac{1}{16\pi G}f(R) + L_m\right)d^4x,$$

Where $f(R)$ is the general function of the Ricci scalar and where $L_m$ is the matter Lagrangian. The variation of the action concerning the metric gives the following equations:

$$F(R)R_{ij} - \frac{1}{2}f(R)g_{ij} - \nabla_i\nabla_j F(R) + g_{ij}\Box F(R) = kT_{ij},$$

Where $F(R) = \frac{df}{dR}$ and where $\Box = \nabla^i\nabla_j,\nabla^i$ is the covariant derivative? Contracting field equation (3), we obtain

$$F(R)R - 2f(R) + 3\Box F(R) = kT,$$

Using $(4)$ in $(3)$, the field equations take the form

$$F(R)R_{jj} - \nabla_i\nabla_j F(R) - kT_{ij} = g_{ij}\left(\frac{F(R)R - \Box F(R) - kT}{4}\right),$$

Equation $(4)$ is an important relationship between $f(R)$ and $F(R)$, which will be used to simplify the field equations and evaluate $f(R)$.

The energy-momentum tensor for matter and GGPDE are respectively given by

$$T_{ij} = \text{diag}[1,0,0,0]\rho_m,$$

$$\bar{T}_{ij} = diag[1, -p_G, -p_G, -p_G],$$

$$\bar{T}_{ij} = diag[1, -\omega_G, -\omega_G, -\omega_G]\rho_G,$$

Where $\rho_m, \rho_G$ are the energy densities of matter and GGPDE respectively? $p_G$ is the pressure of the GGPDE whereas $\omega_G$ is the EoS parameter of the GGPDE.

Einstein's field equation (5) for metric (1) yields the following equations.

$$F\left(\frac{\ddot{A}}{A} + \frac{\dot{A}^2 + \delta}{A^2} + \frac{\dot{A}\dot{B}}{AB} - \frac{B^2}{2A^4}\right) + \frac{1}{2}f(R) - \left(\frac{\dot{A}}{A} + \frac{\dot{B}}{B}\right)\dot{F} - \ddot{F} = -\omega_G\rho_G,$$

$$F\left(\frac{\ddot{B}}{B} + \frac{2\dot{A}\dot{B}}{AB} + \frac{B^2}{2A^4}\right) + \frac{1}{2}f(R) - \frac{2\dot{A}}{A}\dot{F} - \ddot{F} = -\omega_G\rho_G,$$

$$F\left(\frac{2\ddot{A}}{A} + \frac{\ddot{B}}{B}\right) + \frac{1}{2}f(R) - \left(\frac{2\dot{A}}{A} + \frac{\dot{B}}{B}\right)\dot{F} = -(\rho_m + \rho_G),$$

Here the overhead 'dot' denotes differentiation concerning't'. When $\delta = 0, -1, +1$ the field equations (9) - (11) correspond to Bianchi type II, VIII, and IX universes.

The energy conservation equation is

$$\dot{\rho}_m + \dot{\rho}_G + 3H(\rho_m + \rho_G + p_G) = 0,$$

Where overhead (.) denotes differentiation w. r. to cosmic time t.

Throughout the study, we considered both the noninteracting and interacting DMs and GGPDE.

The continuity equation for DM and GGPDE, where the DM component interacts with the GGPDE component through an interaction term *Q*, is as follows:

$$\dot{\rho}_m + 3H\rho_m = Q,$$

$$\dot{\rho}_{DE} + 3H(\rho_G + p_G) = -Q,$$

Where $Q > 0$ indicates that energy flows from the GGPDE to the DM, $Q < 0$ indicates that energy flows in opposite directions and $Q = 0$ represents the noninteracting scenario. In general, $Q$ is inversely proportional to time. Proposed

$$Q = 3bH\rho_m,$$

Where $b > 0$ is the coupling constant?

**III. Solutions of the field equations**

In this case, the set of equations (9) - (11) forms a system of three independent equations with unknowns: $A, B, f(R), \omega_G, \rho_G,$ and $\rho_m$. Hence, to find a determinate solution to these highly nonlinear differential equations, we use the following physically viable conditions:

The shear scalar $\sigma$ is proportional to the scalar expansion $\theta$, which leads to a relationship between the metric potentials, thus,

$$A = B^{\xi},$$

Where $\xi \neq 0$ is a constant and preserves the anisotropic character of the space-time

$F(R)$ The theory of gravity is equivalent to the scalar-tensor theory of gravity, which is incompatible with the solar system test of general relativity, as long as the scalar field propagates over solar system scales Chiba et al.. The power law relationship between the scalar field and average scale factor has already been used by Johari and Sudarshan in the context of FRW models with bulk viscosity in Brans-Dicke theory. However, Uddin et al., have established a result in the context of $F(R)$ theory of gravity, which shows that

$$F(R)\ \alpha\ \left(a(t)\right)^m,$$

Where m is an arbitrary constant. Thus, the power relationships between $F$ and the emergent scenario is given by

$$F(R) = F_0 \left(a(t)\right)^m,$$

Where $F_0$ is a proportionality constant?

(i) We consider an emergent scenario

$$a(t) = a_0(\lambda + e^{\mu t})^{\beta},$$

Where $\lambda, \beta$ and $\mu$ are positive constants. We choose $a_0 > 0$ and $\lambda > 0$ so that initial singularity is avoided. The solution gives rise to inflation and radiation dominance, with the subsequent transition from decelerating to accelerating the universe phase. The emergent scale factor is defined as

$$a(t) = V^{\frac{1}{3}} = \left(A^2 B f(\theta)\right)^{\frac{1}{3}},$$

The energy density of the GGPDE is given by

$$\rho_G = \left(\tau H + \eta H^2\right)^u,$$

Where u is the PDE parameter.

Additionally, the general mean Hubble's parameter$(H)$ is used to describe the volumetric expansion rate of the cosmos.

$$H = \frac{1}{3}\sum_{i=1}^{3} H_i = \frac{1}{3}\left(H_x + H_y + H_z\right),$$

Where $H_x, H_y, H_z$ are directional Hubble parameters? The directional Hubble parameter of space-time is

$$H_x = \frac{A}{A}, H_y = H_z = \frac{C}{C}.$$

From equations (27), (28), and (29) we obtain

$$H = \frac{\dot{a}}{a},$$

We examine the mean anisotropy parameter$(A_m)$ to determine whether the model approaches isotropy.

$$A_m = \frac{1}{3}\sum_{i=1}^{3}\left(\frac{H_i}{H} - 1\right)^2$$

The expansion scalar$(\theta)$ and the shear scalar $(\sigma^2)$ are defined as

$$\theta = 3H,$$

$$\sigma^2 = \frac{3}{2}A_m H^2.$$

The deceleration parameter is defined as

$$q = -\frac{a\ddot{a}}{\dot{a}^2} = -1 + \frac{d}{dt}\left(\frac{1}{H}\right).$$

Where $f(\theta) = 1, cosh\theta$ and $sin\theta$ for the Bianchi-type II, VIII and IX spaces respectively.

From equations (18) and (19) the function $F(R)$ becomes

$$F(R) = F_0 \left(a_0(\lambda + e^{\mu t})^{\beta}\right)^m,$$

The spatial volume V is given by

$$V = a^3 = \left(A^2 B f(\theta)\right),$$

Where $a$ is an emergent scale factor?
The Hubble parameter is calculated as

$$H = \frac{3\beta\mu e^{\mu t}}{(\lambda + e^{\mu t})},$$

$$V = \{a_0(\lambda + e^{\mu t})^{\beta}\}^3,$$

$$q = -1 + \frac{3\beta\mu t e^{\mu t}}{\lambda},$$

$$A_m = \frac{1}{3}\left[\frac{6\xi^2 + 4\xi + 2}{(1 + 2\xi)}\right],$$

$$\sigma^2 = \frac{(3\beta\mu e^{\mu t})^2(3\xi^2 + 2\xi + 1)}{(1 + 2\xi)^2(\lambda + e^{\mu t})^2},$$

$$\theta = \frac{9\beta\mu e^{\mu t}}{(\lambda + e^{\mu t})},$$

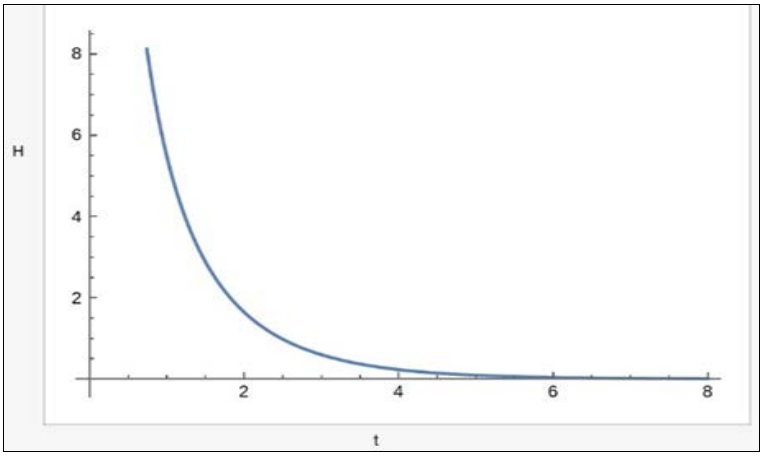


**Fig 1:** Plot of H vs t

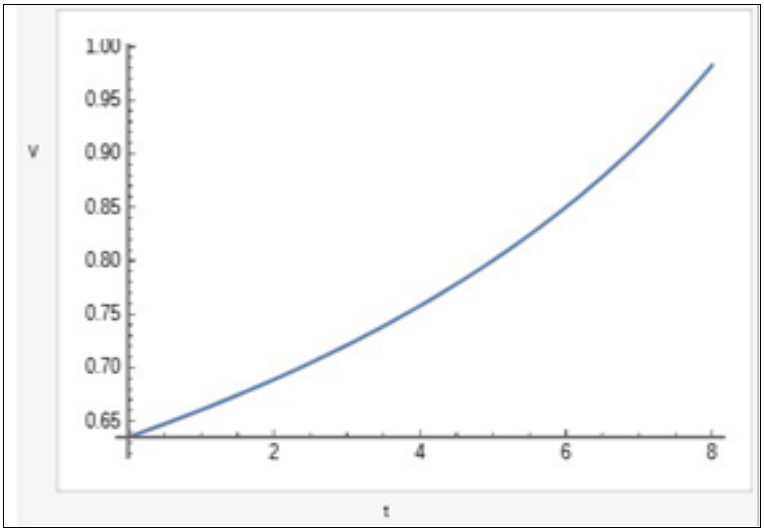


**Fig 2:** Plot of V vs t

We observed from Fig.1 that the mean Hubble parameter was large in the early eras but decreased periodically, so the expansion rate of the universe slowed.

Observe from Fig. 2. At the initial time when t = 0, the volume becomes closer to zero, but with increasing time, the volume increases.

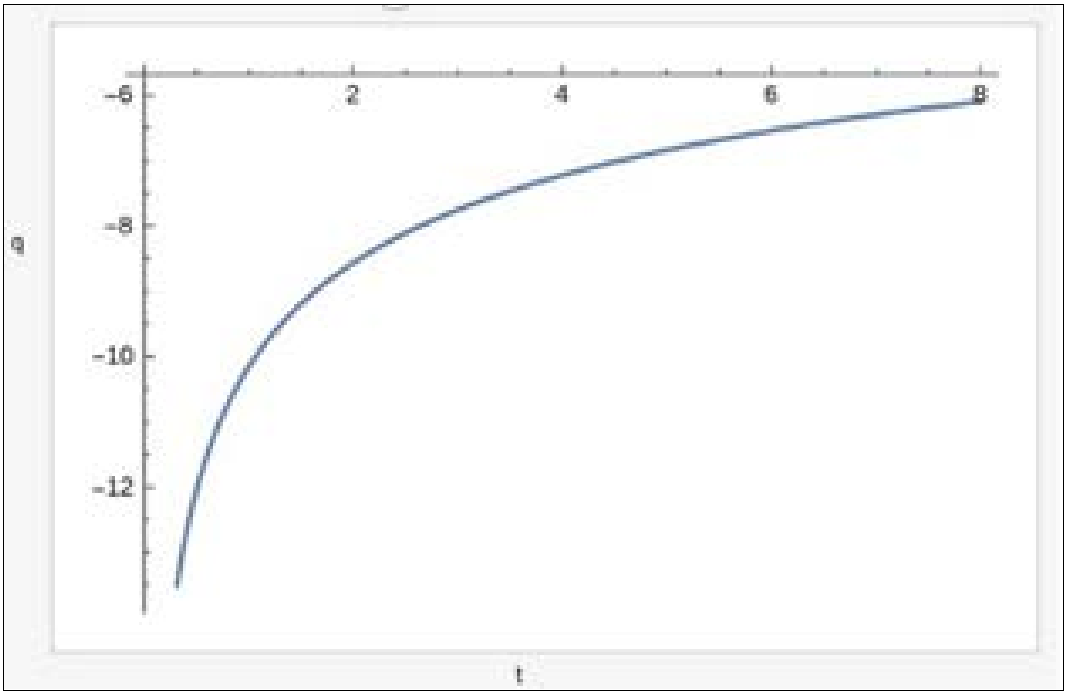


**Fig 3:** Plot of q vs t

From fig. 3 the deceleration parameter is negative throughout cosmic evolution indicating that the universe shows accelerated expansion.

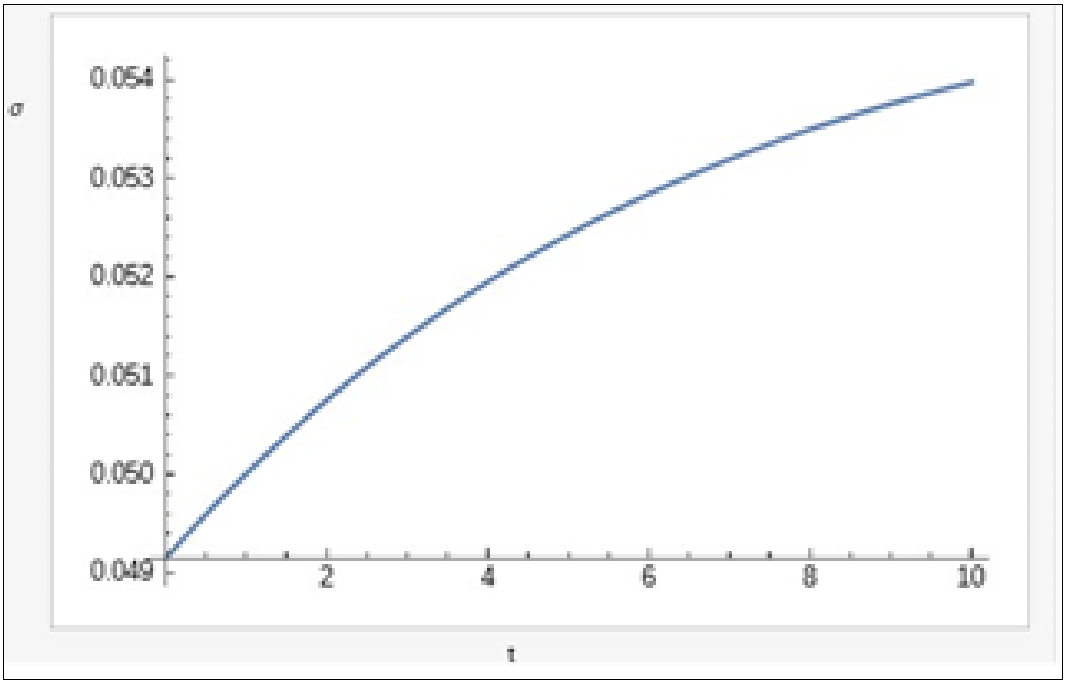


**Fig 4:** plot of σ vs t

Fig. 4 shows that at the initial time expansion, the shear becomes low and gradually increases with increasing time expansion scale.

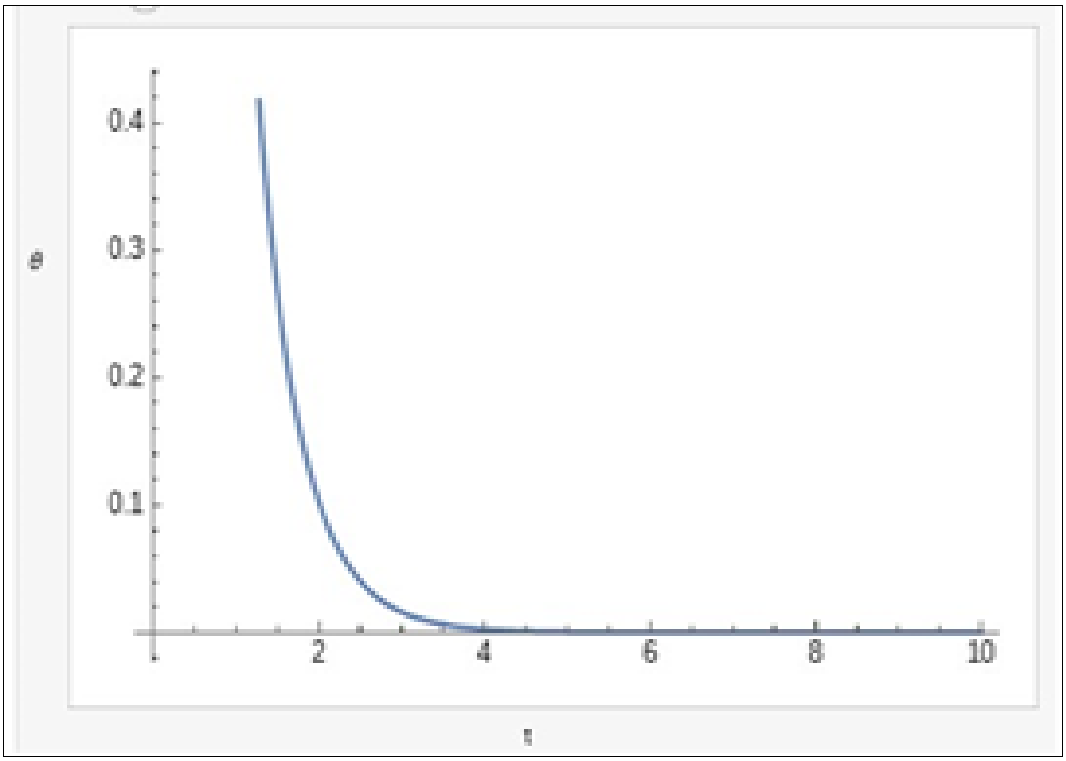


**Fig 5:** Plot of $\theta$ vs t

Fig. 5. shows that at the initial time expansion, the expansion scalar becomes high and gradually decreases with increasing time expansion scale.

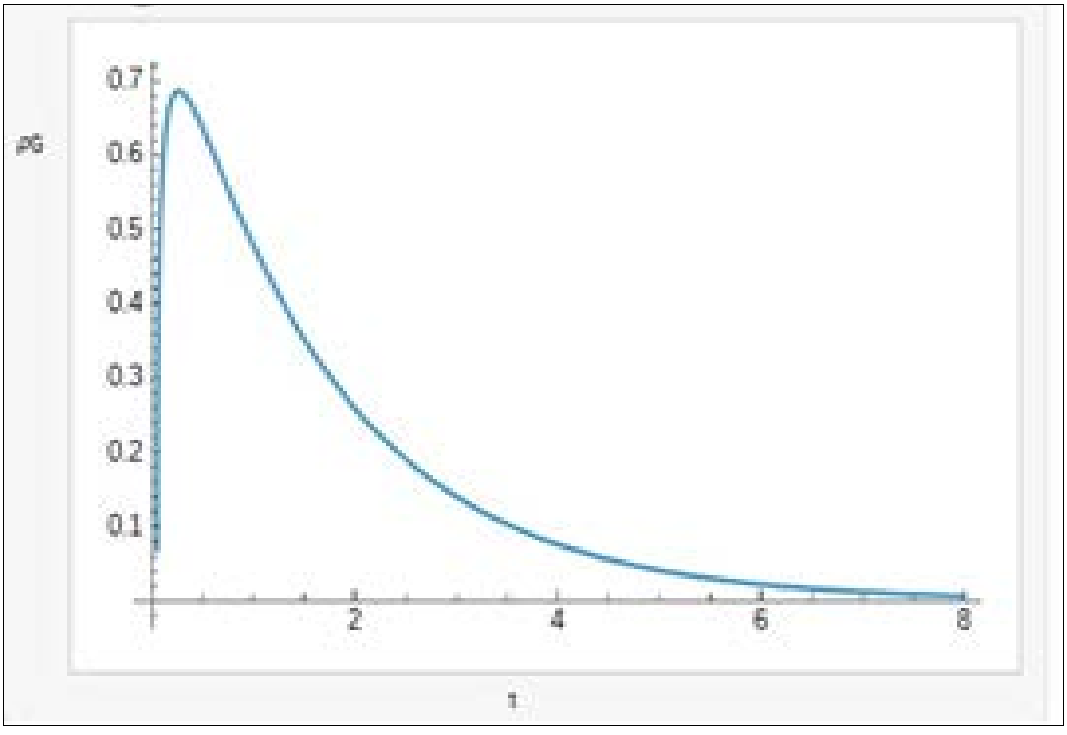


**Fig 6:** Plot of $\rho_G$ vs t

In Fig. 6 the GGPDE density versus cosmic time t is depicted graphically. This is evidence that the GGPDE has a positive effect on density, which decreases with increasing time.

**IV. No interacting model**

The energy conservation equation for the DM is

$$\dot{\rho}_m + 3H\rho_m = 0,$$

Using equation (31) in (38), we obtain

$$\rho_m = \frac{\rho_0}{(\lambda + e^{\mu t})^{3\beta}},$$

Where $\rho_0$ is a constant of integration?
The energy conservation equation for GGPDE is

$$\dot{\rho}_G + 3H(\rho_G + p_G) = 0, \quad p_G = \omega_G \rho_G,$$

From (39) and (11), we obtain

$$f(R) = 2\left(\begin{array}{c}\dfrac{3\beta\mu e^{\mu t}}{\lambda + e^{\mu t}} - F_0\left\{a_0^m[\lambda + e^{\mu t}]^{\beta m}\right\}\dfrac{\begin{array}{c}(6\beta\xi\mu^2 e^{\mu t}(3\xi\beta e^{\mu t} + 2\lambda\xi + \lambda) \\ +3\beta\mu^2 e^{\mu t}(3\beta e^{\mu t} + 2\lambda\xi + \lambda))\end{array}}{(1+2\xi)^2(\lambda + e^{ut})^2} \\ -\rho_0(\lambda + e^{\mu t})^{-3\beta} - \left[\dfrac{\tau\beta\mu}{\lambda + e^{\mu t}} + \eta\left(\dfrac{\beta\mu}{\lambda + e^{\mu t}}\right)^2\right]^u\end{array}\right),$$

$$p_G = -\left(\begin{array}{c}F_0\left[a_0^m(\lambda + e^{\mu t})^{\beta m}\right]\left[\begin{array}{c}\left(\dfrac{3\beta\mu^2 e^{\mu t}(3\beta e^{\mu t} + 2\lambda\xi + \lambda) + 18\beta^2\mu^2 e^{2\mu t}\xi}{(1+2\xi)^2(\lambda + e^{ut})^2}\right) + \\ \dfrac{1}{2}\left(\dfrac{f(\theta)}{a_0^3(\lambda + e^{ut})^{3\beta}}\right)^{\frac{2\xi}{1+2\xi}}\end{array}\right] \\ -\dfrac{6\beta\xi\mu e^{\mu t}}{(1+2\xi)(\lambda + e^{\mu t})}F_0\left[a_0^m e^{\mu t}\beta m\mu(\lambda + e^{\mu t})^{\beta m - 1}\right] \\ -F_0\left[a_0^m e^{\mu t}\beta m\mu^2(\lambda + e^{\mu t})^{\beta m - 2}(\lambda + \beta m e^{\mu t})\right] \\ +\left(\begin{array}{c}\dfrac{3\beta\mu e^{\mu t}}{\lambda + e^{\mu t}} - F_0\left\{a_0^m[\lambda + e^{\mu t}]^{\beta m}\right\}\dfrac{\begin{array}{c}(6\beta\xi\mu^2 e^{\mu t}(3\xi\beta e^{\mu t} + 2\lambda\xi + \lambda) \\ +3\beta\mu^2 e^{\mu t}(3\beta e^{\mu t} + 2\lambda\xi + \lambda))\end{array}}{(1+2\xi)^2(\lambda + e^{ut})^2} \\ -\rho_0(\lambda + e^{\mu t})^{-3\beta} - \left[\dfrac{\tau\beta\mu}{\lambda + e^{\mu t}} + \eta\left(\dfrac{\beta\mu}{\lambda + e^{\mu t}}\right)^2\right]^u\end{array}\right)\end{array}\right),$$

The GGPDE density is calculated as

$$\rho_G = \left[\frac{\tau\beta\mu}{\lambda + e^{\mu t}} + \eta\left(\frac{\beta\mu}{\lambda + e^{\mu t}}\right)^2\right]^u,$$

$$\omega_G = -\frac{\left(\begin{array}{c}F_0\left[a_0^m(\lambda+e^{\mu t})^{\beta m}\right]\left[\begin{array}{c}\left(\dfrac{3\beta\mu^2 e^{\mu t}(3\beta e^{\mu t}+2\lambda\xi+\lambda)+18\beta^2\mu^2 e^{2\mu t}\xi}{(1+2\xi)^2(\lambda+e^{ut})^2}\right)+ \\ \dfrac{1}{2}\left(\dfrac{f(\theta)}{a_0^3(\lambda+e^{ut})^{3\beta}}\right)^{\frac{2\xi}{1+2\xi}}\end{array}\right] \\ -\dfrac{6\beta\xi\mu e^{\mu t}}{(1+2\xi)(\lambda+e^{\mu t})}F_0\left[a_0^m e^{\mu t}\beta m\mu(\lambda+e^{\mu t})^{\beta m-1}\right] \\ -F_0\left[a_0^m e^{\mu t}\beta m\mu^2(\lambda+e^{\mu t})^{\beta m-2}(\lambda+\beta m e^{\mu t})\right] \\ +\left(\begin{array}{c}\dfrac{3\beta\mu e^{\mu t}}{\lambda+e^{\mu t}} - F_0\left\{a_0^m[\lambda+e^{\mu t}]^{\beta m}\right\}\dfrac{\begin{array}{c}(6\beta\xi\mu^2 e^{\mu t}(3\xi\beta e^{\mu t}+2\lambda\xi+\lambda) \\ +3\beta\mu^2 e^{\mu t}(3\beta e^{\mu t}+2\lambda\xi+\lambda))\end{array}}{(1+2\xi)^2(\lambda+e^{ut})^2} \\ -\rho_0(\lambda+e^{\mu t})^{-3\beta} - \left[\dfrac{\tau\beta\mu}{\lambda+e^{\mu t}} + \eta\left(\dfrac{\beta\mu}{\lambda+e^{\mu t}}\right)^2\right]^u\end{array}\right)\end{array}\right)}{\left[\dfrac{\tau\beta\mu}{\lambda+e^{\mu t}} + \eta\left(\dfrac{\beta\mu}{\lambda+e^{\mu t}}\right)^2\right]^u},$$

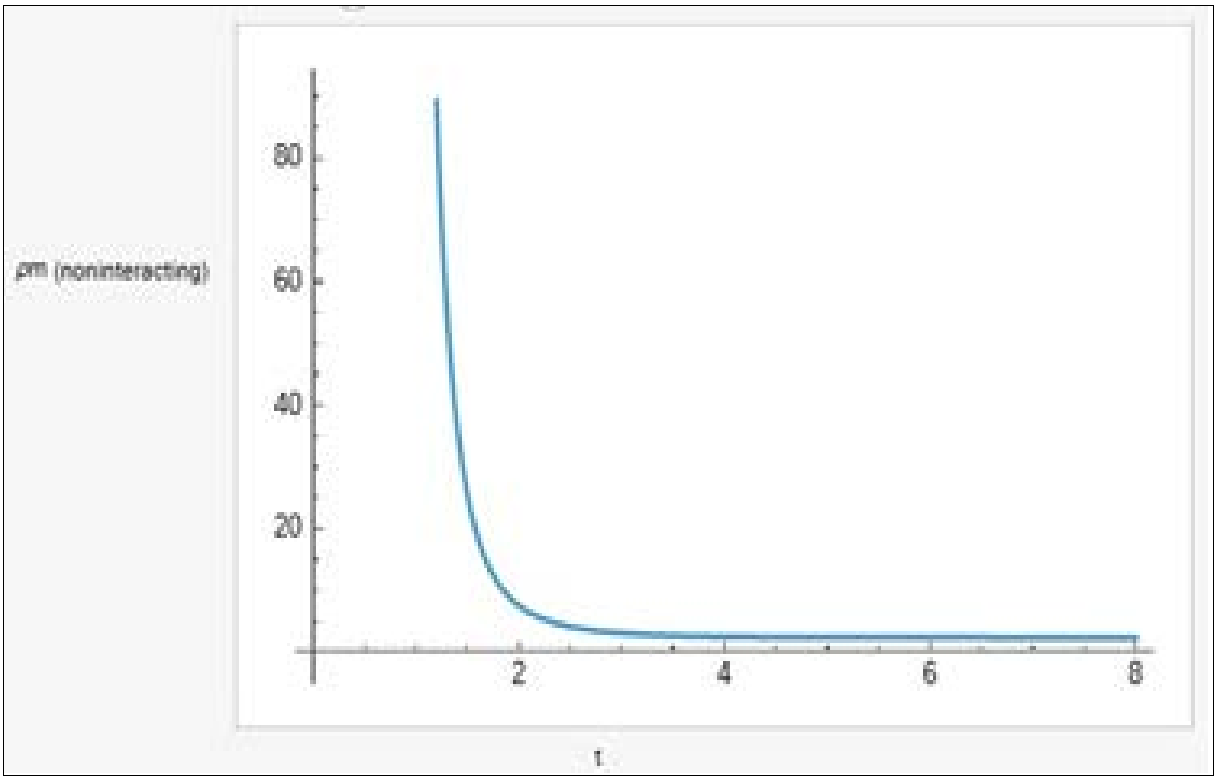


**Fig 7:** Plot of $\rho_m$ vs t

Fig. 7 shows that the matter density becomes high at the initial time expansion and exponentially decreases with increasing time.

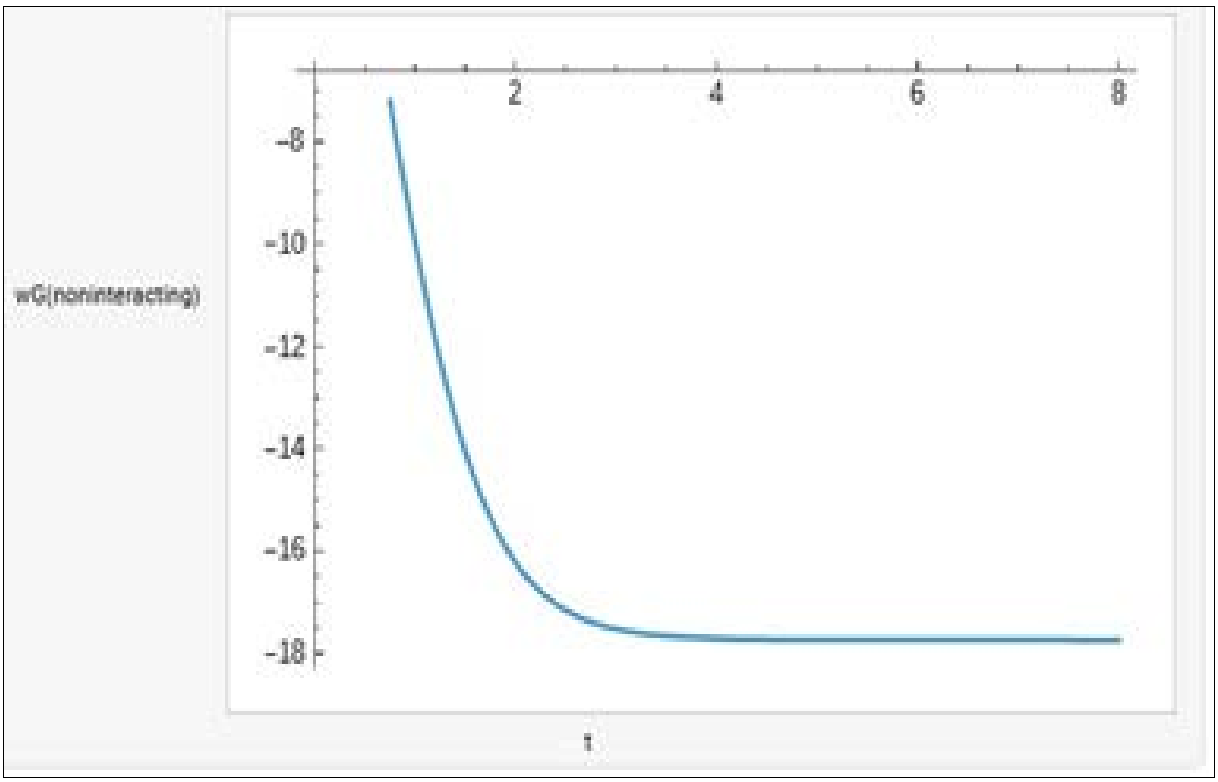


**Figure 8:** Plot of $\omega_G$ vs t

In Fig. 8 the GGPDE EoS parameter versus cosmic time t is depicted graphically. This is evidence that DE exerts a negative EoS parameter throughout the universe's expansion.

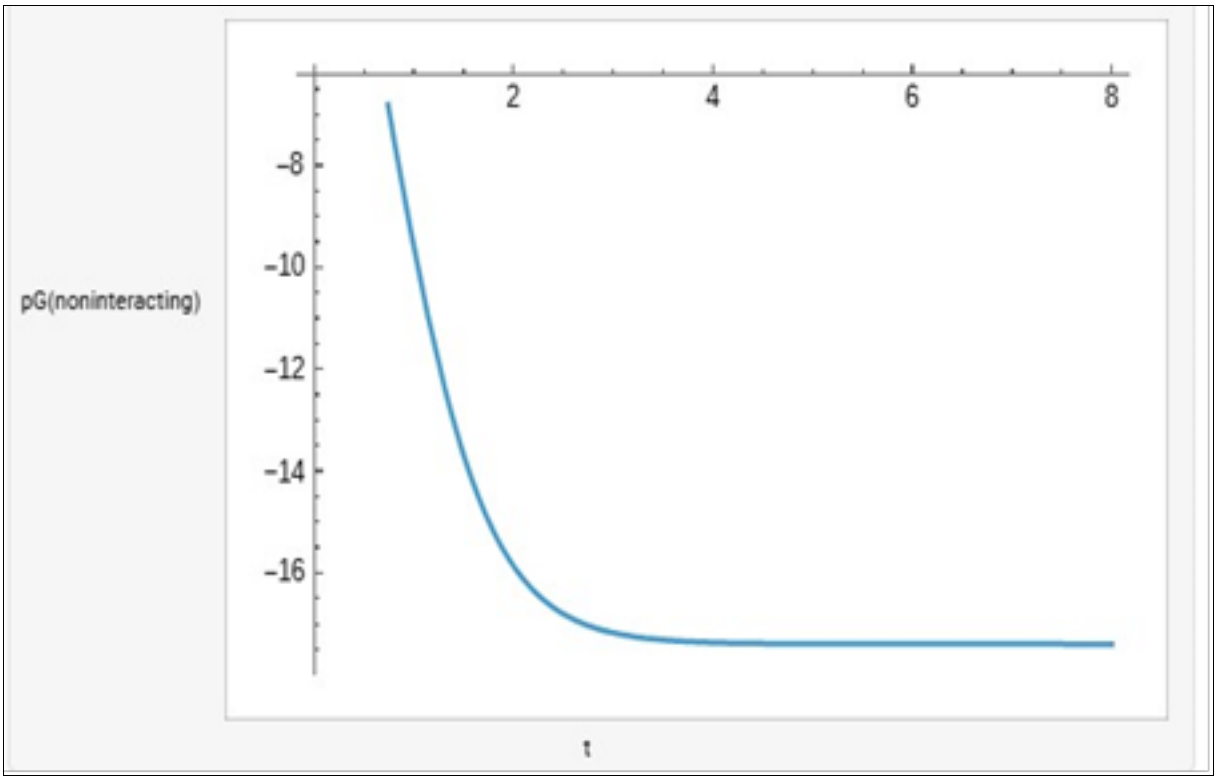


**Fig 9:** Plot of $p_G$ vs t

In Fig. 9 the GGPDE pressure versus cosmic time t is depicted graphically. This is evidence that GGPDE exerts a negative pressure throughout the universe's expansion.

**V. Interacting model**

The energy conservation equation for the DM is

$$\dot{\rho}_m + 3H\rho_m = 3bH\rho_m$$

Using (31) in (45) we obtain

$$\rho_m = \rho_0{}'(\lambda + e^{\mu t})^{3\beta(b-1)},$$

Where $\rho_0$ is a constant of integration?

The energy conservation equation for GGPDE is

$$\dot{\rho}_G + 3H(\rho_G + p_G) = 3bH\rho_m,$$

From (39) and (11) we obtain

$$f(R) = 2\left(\begin{array}{c} \dfrac{3\beta\mu e^{\mu t}}{\lambda + e^{\mu t}} - F_0\{a_0^m[\lambda + e^{\mu t}]^{\beta m}\}\dfrac{(6\beta\xi\mu^2 e^{\mu t}(3\xi\beta e^{\mu t} + 2\lambda\xi + \lambda)}{+3\beta\mu^2 e^{\mu t}(3\beta e^{\mu t} + 2\lambda\xi + \lambda))} \\ -\rho_0{}'(\lambda + e^{\mu t})^{3\beta(b-1)} - \left[\dfrac{\tau\beta\mu}{\lambda + e^{\mu t}} + \eta\left(\dfrac{\beta\mu}{\lambda + e^{\mu t}}\right)^2\right]^u \end{array}\right),$$

$$p_G = -\left( \begin{array}{c} F_0\left[a_0^m(\lambda+e^{\mu t})^{\beta m}\right]\left[\left(\frac{3\beta\mu^2 e^{\mu t}(3\beta e^{\mu t}+2\lambda\xi+\lambda)+18\beta^2\mu^2 e^{2\mu t}\xi}{(1+2\xi)^2(\lambda+e^{\mu t})^2}\right)+\right. \\ \left.\frac{1}{2}\left(\frac{f(\theta)}{a_0^3(\lambda+e^{\mu t})^{3\beta}}\right)^{\frac{2\xi}{1+2\xi}}\right] \\ -\frac{6\beta\xi\mu e^{\mu t}}{(1+2\xi)(\lambda+e^{\mu t})}F_0\left[a_0^m e^{\mu t}\beta m\mu(\lambda+e^{\mu t})^{\beta m-1}\right] \\ -F_0\left[a_0^m e^{\mu t}\beta m\mu^2(\lambda+e^{\mu t})^{\beta m-2}(\lambda+\beta m e^{\mu t})\right] \\ +\left(\begin{array}{c}\frac{3\beta\mu e^{\mu t}}{\lambda+e^{\mu t}}-F_0\left\{a_0^m[\lambda+e^{\mu t}]^{\beta m}\right\}\frac{(6\beta\xi\mu^2 e^{\mu t}(3\xi\beta e^{\mu t}+2\lambda\xi+\lambda)}{+3\beta\mu^2 e^{\mu t}(3\beta e^{\mu t}+2\lambda\xi+\lambda))}{(1+2\xi)^2(\lambda+e^{\mu t})^2} \\ -\rho_0{}'(\lambda+e^{\mu t})^{3\beta(b-1)}-\left[\frac{\tau\beta\mu}{\lambda+e^{\mu t}}+\eta\left(\frac{\beta\mu}{\lambda+e^{\mu t}}\right)^2\right]^u\end{array}\right) \end{array}\right),$$

Using equations (31) and (41) in (47),

$$\omega_G = -\frac{\left( \begin{array}{c} F_0\left[a_0^m(\lambda+e^{\mu t})^{\beta m}\right]\left[\left(\frac{3\beta\mu^2 e^{\mu t}(3\beta e^{\mu t}+2\lambda\xi+\lambda)+18\beta^2\mu^2 e^{2\mu t}\xi}{(1+2\xi)^2(\lambda+e^{\mu t})^2}\right)+\right. \\ \left.\frac{1}{2}\left(\frac{f(\theta)}{a_0^3(\lambda+e^{\mu t})^{3\beta}}\right)^{\frac{2\xi}{1+2\xi}}\right] \\ -\frac{6\beta\xi\mu e^{\mu t}}{(1+2\xi)(\lambda+e^{\mu t})}F_0\left[a_0^m e^{\mu t}\beta m\mu(\lambda+e^{\mu t})^{\beta m-1}\right] \\ -F_0\left[a_0^m e^{\mu t}\beta m\mu^2(\lambda+e^{\mu t})^{\beta m-2}(\lambda+\beta m e^{\mu t})\right] \\ +\left(\begin{array}{c}\frac{3\beta\mu e^{\mu t}}{\lambda+e^{\mu t}}-F_0\left\{a_0^m[\lambda+e^{\mu t}]^{\beta m}\right\}\frac{(6\beta\xi\mu^2 e^{\mu t}(3\xi\beta e^{\mu t}+2\lambda\xi+\lambda)}{+3\beta\mu^2 e^{\mu t}(3\beta e^{\mu t}+2\lambda\xi+\lambda))}{(1+2\xi)^2(\lambda+e^{\mu t})^2} \\ -\rho_0{}'(\lambda+e^{\mu t})^{3\beta(b-1)}-\left[\frac{\tau\beta\mu}{\lambda+e^{\mu t}}+\eta\left(\frac{\beta\mu}{\lambda+e^{\mu t}}\right)^2\right]^u\end{array}\right) \end{array}\right)}{\left[\frac{\tau\beta\mu}{\lambda+e^{\mu t}}+\eta\left(\frac{\beta\mu}{\lambda+e^{\mu t}}\right)^2\right]^u},$$

in all the above expressions $f(\theta) = 1, cosh\theta, and \ \ sin\theta$ for Bianchi type-II, VIII and IX space times, respectively. Now, metric (1) can be written as

$$ds^2 = -dt^2 + \left(\left(\frac{a_0^3(\lambda+e^{ut})^{3\beta}}{f(\theta)}\right)^{\frac{\xi}{1+2\xi}}\right)^2 [d\theta^2 + f^2(\theta)\,d\phi^2] + \left(\left(\frac{a_0^3(\lambda+e^{ut})^{3\beta}}{f(\theta)}\right)^{\frac{1}{1+2\xi}}\right)^2 [d\psi + h(\theta)\,d\phi]^2,$$

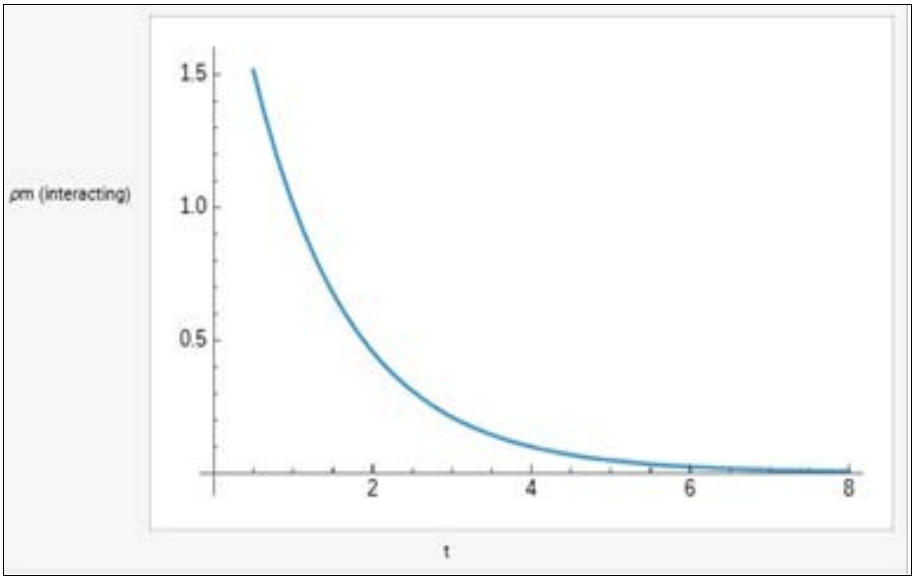


**Fig 10:** Plot of $\rho_m$ vs t

Fig 10. The matter density decreases with increasing time.

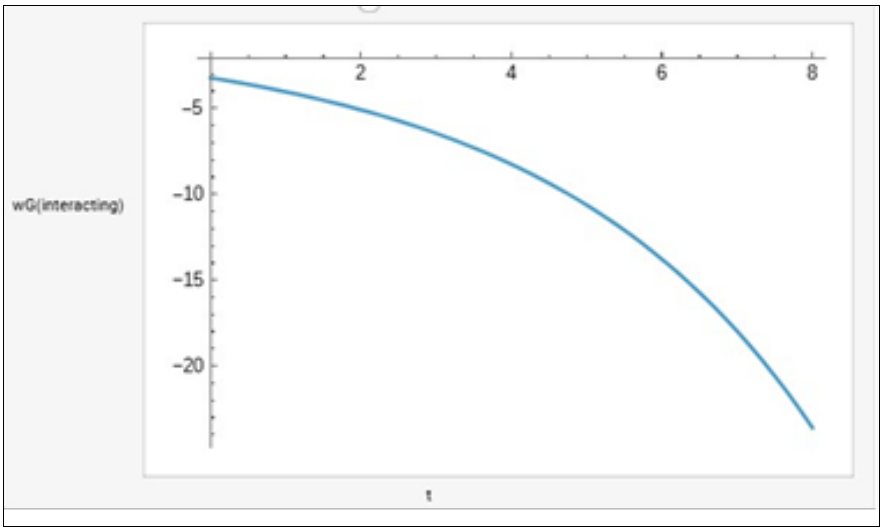


**Fig 11:** Plot of $\omega_G$ vs t

Fig. 11 shows the variation in the EoS parameter of the GGPDE with respect to time. This is evidence that DE exerts a negative Eos parameter throughout the universe's expansion and decreases with increasing time.

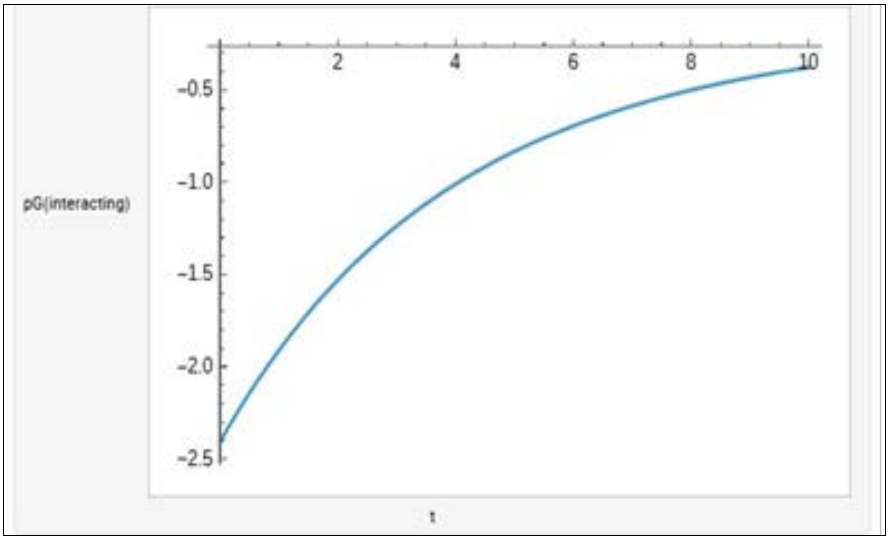


**Fig 11:** Plot of $p_G$ vs t

Fig. 12 shows the variation in the pressure of GGPDE with respect to time. This is evidence that GGPDE exerts negative pressure throughout the universe's expansion and increases with increasing time.

## Conclusion

This investigation is about the determination of Bianchi-type II, VIII and IX HDE cosmological models with emergent scenarios of scale factor in $f(R)$ gravity. We have obtained cosmological models corresponding to HDE using some physically viable conditions.

We observed that Fig. 1. The mean Hubble parameter was large in the early eras but decreased periodically, so the universe's expansion rate slowed. Fig. 2. At the initial time when t = 0, the volume becomes closer to zero, but with increasing time, the volume increases. Fig. 3 shows that the deceleration parameter shows a highly negative value at the initial time and it decreases as the cosmic time increases. This indicates that the universe is accelerating throughout the evolution of the universe. Fig. 4 shows that at the initial time expansion, the shear becomes low and gradually increases with increasing time expansion scale. Fig. 5 shows that at the initial time expansion, the expansion scalar becomes high and gradually decreases with increasing time expansion scale. In Fig. 6 the GGPDE density versus cosmic time t is depicted graphically. This is evidence that the GGPDE has a positive effect on density, which decreases with increasing time. We observed from the noninteracting model that Fig. 7 shows that the matter density becomes high at the initial time expansion and exponentially decreases with increasing time. In Fig. 8 the GGPDE EoS parameter versus cosmic time t is depicted graphically. This is evidence that DE exerts a negative EoS parameter throughout the universe's expansion. In Fig. 9 the GGPDE pressure versus cosmic time t is depicted graphically. This is evidence that DE exerts a negative pressure throughout the universe's expansion and from the interacting model Fig. 10. The matter density decreases with increasing time. Fig. 11 shows the variation in the EoS parameter of the GGPDE with respect to time. This is evidence that DE exerts a negative Eos parameter throughout the universe's expansion and decreases with increasing time. Fig. 12 shows the variation in the pressure of GGPDE with respect to time. This is evidence that GGPDE exerts negative pressure throughout the universe's expansion and increases with increasing time.

The interesting features that we have found in this paper are that both interacting and noninteracting models behave like cosmological constants. This work presented here may give a better understanding of the evolution of the universe and a satisfactory result on GGPDE which are good in agreement with present-day observations.

## References


1. Riess AVF, Adam G. Observational evidence from supernovae for an accelerating universe and a cosmological constant. Astron. 1998;1009-1038.
2. Perlmutter S. Discovery of a supernova explosion at half the age of the universe. Nature. 1998;391:51-54.
3. Bennett CL. First-year Wilkinson Microwave Anisotropy Probe (WMAP) observation: preliminary maps and basic results. *Astrophysics*. 2003;148.
4. Spergel DN. First Wilkinson Microwave Anisotropy Probe (WMAP) observations: determination of cosmological parameters. Astrophysics. 2003;148:175-194.
5. Tegmark M. Cosmological parameters from SDSS and WMAP. Phys Rev D. 2004;69:103501.
6. Barali J. Dynamics of generalized ghost pilgrim dark energy in general relativity. Bulgarian J Phys. 2023;50:1-15.
7. Miller AD. Improved retroviral vectors for gene transfer and expression. Astrophysics. 1989;524:980-990.
8. Kamenshchik AY. An alternative to quintessence. Phys Lett B. 2001;511:265-8.
9. Hsu. Entropy bounds and dark energy. Phys Lett B. 2004;594:13-16.
10. Li M. A model of holographic dark energy. Phys Lett B. 2004;603.
11. Hao WA. Pilgrim dark energy. Class Quantum Grav. 2012;29.
12. Santhi MV. Some Bianchi type bulk viscous string cosmological models in f(R) gravity. *J Phys*. 2019;1344.
13. Sharif M. Anisotropic fluid and Bianchi type III model in f(R) gravity. Phys Lett B. 2011;697:1-6.
14. Aditya UPY. Plane-symmetric dark energy model with a massive scalar field. New Astron. 2021;12:339.
15. Shamir M. Some Bianchi type cosmological models in f(R) gravity. Astrophys Space Sci. 2010;330:183.
16. Yılmaz İ. Quark and strange quark matter in f(R) gravity for Bianchi type I and V space-times. Gen Relativ Gravit. 2012;44:2313-2328.
17. Reddy DRK. Vacuum solutions of Bianchi type-I and V models in f(R) gravity with a special form of deceleration parameter. Int J Sci Adv Technol. 2014;4:23.
18. Amir MJ. Locally rotationally symmetric vacuum solutions in f(R) gravity. Int J Theor Phys. 2013;53:773.
19. Yerramsetti. Nonvacuum plane symmetric universe in f(R) gravity. Results Phys. 2018;12.
20. Saha B. Some remarks on Bianchi type-II, VIII, and IX models. Gravitation Cosmol. 2013.
21. Katore SD. Bianchi Type II VIII and IX string cosmological models in f(R) gravity. Int J Theor Phys. 2015;54:2700-11.
22. Singh T. Bianchi type-II, VIII, and IX in certain new theories of gravitation. Astrophys Space Sci. 1992;191:61-88.
23. Vijaya Santhi TCM. Tsallis holographic dark energy in Bianchi type–II, VIII and IX universes. Astrophys Space Sci. 2023;368.
24. Karagiorgos TPA. Quantum cosmology of Bianchi VIII, IX LRS geometries. J Cosmol Astropart Phys. 2019;April.
25. Urban F. The cosmological constant from the QCD Veneziano ghost. Phys Lett B. 2010;688(1):9-12.
26. Urban F. The QCD nature of dark energy. Nucl Phys B. 2010;835(1-2):135-173.
27. Ohta N. Dark energy and QCD ghost. Phys Lett B. 2011;695:641.
28. Cai R. Notes on ghost dark energy. Phys Rev D. 2011;84(12):123501.
29. Zhitnitsky A. Gauge fields and ghosts in Rindler space. *Phys Rev D*. 2010;82(10):103520.
30. Holdom B. From confinement to dark energy. Phys Lett B. 2011;697(4):351-356.
31. Zhitnitsky A. Contact interaction with horizon and dark energy. Entropy. 2010.

32. Zhitnitsky A. Contact term, its holographic description in QCD and dark energy. Phys Rev D. 1988;6.
33. Maggiore M. Early dark energy from zero-point quantum fluctuations. Phys Lett B. 2011;704(3):102-107.
34. Cai RG, Zhang Y, Wang Y, Zhang Z, Yang T. More on QCD ghost dark energy. Phys Rev D. 2012;86:023511.
35. Bhoyar SR, Ingole YB, Kale AP. Generalized ghost pilgrim dark energy fractal cosmology with observational constraint. Phys Scr. 2024;015026.
36. Wei H. Pilgrim dark energy. Class Quantum Grav. 2012;29:175008.
37. Sharif MJ. Analysis of generalized ghost version of pilgrim dark energy. Astrophys Space Sci. 2014;351:321.
38. Tiwari MSRK. Polytropic bulk viscous cosmological model with variable G and Λ. Open Access Libr J. 2014;1(5).
39. Nojiri S. Different faces of generalized holographic dark energy. Symmetry. 2021;13(6):13060928.
40. Dave RB, Suresh S. Bianchi Type-III string cosmological model with bulk viscous fluid in general relativity. Astrophys Space Sci. 2002;282:461-466.
41. Bhoyar SR. Maximal coupling of Bianchi type-II, VIII and IX space-time with HDE and DM in f(R,T) gravity. Int J Sci Res Phys Appl Sci. 2018;6:139-145.
42. Sotiriou TP. f(R) theories of gravity. Astrophysics. 2008;4.
43. Wei H. Interacting agegraphic dark energy. Eur Phys J. 2009;59:99-105.
44. Collins CB. Exact spatially homogeneous cosmologies. Gen Relativ Gravit. 1980;12:805-823.
45. Chiba T. Solar system constraints to general f(R) gravity. Phys Rev D. 2007;75:12404.
46. Johri VB. BD-FRW cosmology with bulk viscosity. Aust J Phys. 1989;42(2):215-222.
47. Uddin K. Cosmological perturbations in Palatini-modified gravity. Class Quantum Grav. 2007;24(15):3951.